Quantum Electronics **30** (11) 941 – 948 (2000)

INVITED PAPER

PACS numbers: 42.62.Cf; 42.55.Rz; 81.20.Vj
DOI: 10.1070/QE2000v030n11ABEH001825

Extension of potentialities of millisecond pulsed Nd:YAG lasers in the welding technology

S V Kayukov

Abstract. The dependences of the dynamic parameters of the growth of a vapour-gas channel and the depth of the melting zone on the shape of laser pulses and the spatial beam parameters are studied. Based on this study, the requirements are formulated to the characteristics of radiation providing a many-fold increase in the melting depth with respect to the depth that was previously considered as limiting. A new laser setup for deep high-quality welding was built. The role of the buffer volume of a melt in the suppression of ejection of molten metal from the laser-heated region upon deflection of the melt surface is substantiated. An increase in the rate of growth of a vapour-gas channel during an increase in its length (the self-concentration of a heat source) was experimentally observed. At the depths corresponding to the preferential vertical orientation of fluid flows, a large-scale vortex motion of the melt was observed. The dependence of the penetration depth of the melting front on the aperture angle β was experimentally found to have an extremum. The maximum penetration depth was obtained for $\beta = 0.075 - 0.80$ rad. Recommendations for designing pulsed laser technological systems for high-quality welding of metals are formulated.

1. Introduction

The behaviour of metals and alloys under the action of high-power laser radiation with duration exceeding 10^{-8} s and intensity below 10^9 W cm^{-2}, which are typical of pulsed solid-state free-running lasers, can be analysed using the model of an equivalent heat source instead of a laser [1 – 4]. The study of physical processes proceeding during laser heating is stimulated, to a considerable degree, by rich potentialities of its efficient use for solving different technological problems, predominantly those related to melting and evaporation of a material exposed to laser radiation. In particular, the material of details being welded should be heated to temperatures exceeding the melting point, and a common melt bath should be formed.

Of considerable interest are such welding regimes in which the free surface of a melt is strongly deflected and the growth of a vapour-gas channel, which acts as an optical guide transporting laser radiation to a cold bottom, is provided [4]. Under these conditions, the largest depth of the melting zone and the highest efficiency of employment of laser radiation are realised.

The steady-state welding, with a vapour-gas channel that is in equilibrium with the environment, has been studied actively for some years for fundamental and applied purposes [5 – 7]. The deflection of the melt surface, the formation of a vapour-gas channel, and its growth under pulsed heating are accompanied by the displacement of a melt to the surface and the ejection of particles of the melt from the irradiation region. Therefore, it is commonly accepted that millisecond pulsed laser radiation can be used only for welding details of a small thickness (thinner than 2 mm), when welding can be realised without the formation of a vapour-gas channel. Because of this, pulsed technological lasers have not been substantially developed in recent decades. For instance, although the average power and the pulse energy of the RSY 500Y laser from Rofin Sinar Co. or the HL series of lasers from Haas Co. are as high as 500 W and 80 J, respectively, these lasers cannot provide a melting depth more than 2 mm.

If heat is transferred through heat conduction, one can estimate the limiting melting depth z_0 using the expression for the temperature $T(z, t)$ of a semi-infinite body that is heated through the surface $z = 0$ by a constant heat flux q_0 [8]:

$$T(z,t) = \frac{2q_0}{\lambda}\sqrt{\kappa t}\,\mathrm{ierfc}\left(\frac{z}{2\sqrt{\kappa t}}\right), \qquad (1)$$

where λ and κ are the heat conductivity and the thermal conductivity, respectively. Assuming that the surface temperature is equal to the boiling temperature and the temperature at the desired depth z_0 is equal to the melting temperature, one can readily obtain for iron and $t = 0.01$ s from (1) the depth $z_0 \simeq 0.3$ mm. If a laser beam is focused on the surface of a sample into a spot with radius $r = 0.15$ mm, the limiting laser pulse energy W_0 is about 3 J.

Thus, in the case of conductive heat transfer, the melting depth and the energy deposition in a metal are strongly limited. An arbitrary increase in the radiation power, when the free melt surface is strongly deflected and the conditions for the formation of a vapour-gas channel are realised, disturbs the stability of a molten metal and causes the ejection of particles of the melt from the heated region. Because the fluid is ejected under the action of reaction pressure of the metal vapour, which is determined by the surface

S V Kayukov P. N. Lebedev Physics Institute, Samara Branch, Russian Academy of Sciences, Novo-Sadovaya ul. 221, 443011 Samara, Russia

Received 25 January 2000
Kvantovaya Elektronika **30** (11) 941 – 948 (2000)
Translated by A N Kirkin

melt temperature, the shape of a laser pulse should be optimised using the criterion of a constant surface temperature during the action of a laser pulse.

One can illustrate this problem in a simplified version using the model of a semi-infinite body with constant thermal parameters, without accounting for the melting heat. The solution of this problem is well known [8]. For the surface, it can be written in the form

$$T(0,t) = \kappa^{1/2}\lambda^{-1}\pi^{-1/2}\int_0^t \frac{q(y)\mathrm{d}y}{\sqrt{t-y}}. \qquad (2)$$

Let the surface temperature be constant starting with a certain moment of time t_0 [$T(0, t > t_0) = T_0$]. Until this moment the temperature increases, say, linearly with time. In this case, using the solution known for the Abel problem, one can write for the heat flow function

$$q(t) = \begin{cases} \dfrac{2T_0\lambda}{t_0\sqrt{\kappa\pi}}\sqrt{t}, & t < t_0, \\ \dfrac{2T_0\lambda}{t_0\sqrt{\kappa\pi}}\left(\sqrt{t} - \sqrt{t-t_0}\right), & t \geqslant t_0. \end{cases} \qquad (3)$$

Fig. 1 presents the form of the function $q(t)$ (3) and the corresponding temperature of the irradiated surface. However, the assumptions made for obtaining (3) cannot be applied in the case of melting metals to a rather large depth, when convective flows in the melt bath make a large contribution to the heat and mass transfer.

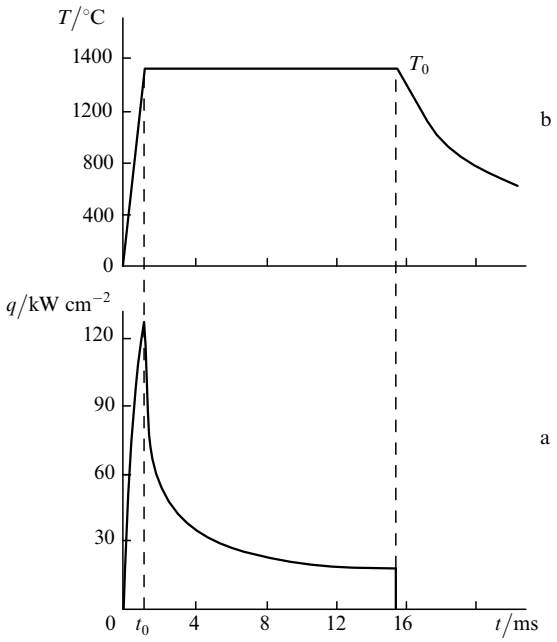

Figure 1. Calculated shape of a radiation pulse providing (a) a constant temperature (b) at the irradiated surface during the interaction time.

This work is aimed at the physical substantiation of the development of pulsed lasers of a new generation for high-quality welding, with the melting depth that is many-fold greater than the limiting depth for lasers of the old generation.

2. Experiment

The experiments were carried out using a laser system built on the basis of a pulsed Nd : YAG laser with two active GP 6.3×100-mm elements. Its distinctive feature is the feasibility of smooth tailoring of the laser pulse shape in a wide range, with pulse length varied from 1.5 to 20 ms. This was realised by dividing a storage capacitor of a power supply into 12 independent sections [9]. All sections were charged to the same voltage, which was specified by a control unit. A pulse shape was controlled by changing independently the capacity and inductance of each section and varying the delay time of the discharge in each section relative to the controlling pulse.

Fig. 2 illustrates the shapes of 12 laser pulses, which are arranged in order of increasing the leading-edge duration. The laser had a stable cavity of length from 42 to 120 cm. with a plane output mirror and a spherical rear mirror ($R = 240$ cm). Using an additional intracavity aperture, we were able to obtain a quality parameter of 2 mm×mrad for a laser beam. The changeable apertures were 1.5, 2.0, 2.5, and 3.8 mm in diameter. The output laser beam was transformed by a telescope with a magnification of 2, 2.5, 4, 5, 6.7, or 13.5 and then focused on a sample by an objective with a focal distance of 10 or 15 cm.

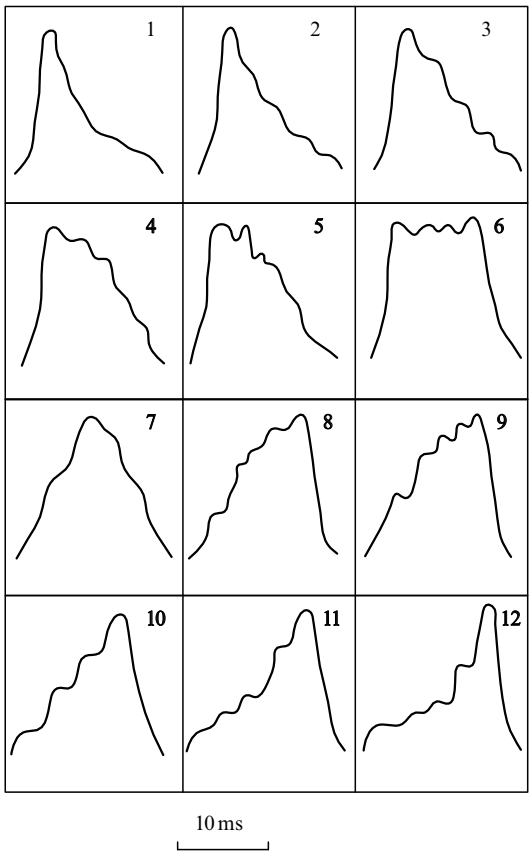

Figure 2. Oscillograms of laser radiation pulses under study.

The diameter d of the focal spot on the surface of a sample and the aperture angle β for the given divergence θ_0 and the aperture A_0 of the incident beam were determined from the relations

$$\beta = K\frac{A_0}{F}, \qquad \frac{d}{2} = \theta_0\frac{F}{K}. \tag{4}$$

The coefficient K, which is equivalent to the telescope magnification, was discretely changed, taking the values 1, 2, 4, 6, 7.2, 8.4, 10.8, and 12.6. Owing to independent changes in the diameter of the intracavity aperture and the coefficient K, we experimentally realised 48 different combinations of the aperture angle β and the radiation divergence θ in the ranges 0.01 rad $< \beta <$ 0.5 rad and 0.08 rad $< \theta <$ 4.0 mrad.

An aperture 1.5 mm in diameter provided lasing on the fundamental TEM_{00} mode throughout the accessible pump range. In the case of a 2.0-mm aperture, laser radiation represented a superposition of modes with indices not greater than unity, and when the aperture diameter was increased above 3 mm, we obtained multimode lasing.

For rapid obtaining data on the shape and size of the melting zone, we determined geometrical parameters of this region by the technique that required no laborious preparation of metallographic sections. Each sample was composed of two polished plane-parallel plates, which were strongly forced against one another in a clamp. Laser radiation was focused onto the joint of the plates on one of the faces of a sample. After the destruction of a sample along the joint, the longitudinal sections of melting zones were visually inspected using Neophot-30 and MBS-9 optical microscopes. As shown in Ref. [10], this technique is not only less laborious, but also provides minimum measurement errors.

The method of determining dynamic characteristics of the growth of a vapour-gas channel [11] is based on the fact that in the case of deep melting, the thickness $x(z)$ of the layer that is bounded by the melting front with the temperature T_m and a certain isotherm T_h is uniquely related to the time of action of a thermal source at the given depth z. For steel, the temperature T_h was taken equal to the lower boundary of the hardening range because the dimensions of the hardening region can be determined with a high accuracy from metallographic sections. Using the experimental dependence of the hardened-layer thickness on the depth $x(z)$, we determined the time $t(z)$ during which the melt existed at the given depth and the velocity $V_f(z)$ at which the melting front moved along the z-axis:

$$t(z) = \frac{1}{\xi}x^2(z), \quad V_f(z) = \frac{\xi}{2}\left(x\frac{dx}{dz}\right)^{-1}, \tag{5}$$

where $\xi = 0.1 - 0.2$ cm^2 s^{-1} is a constant for each individual experiment, which has dimension of thermal conductivity.

We made a series of experiments on high-speed photochronography of the state of the irradiated surface in real time. Using a high-speed VSK-5 camera, we recorded both the specular reflection of the probe radiation of a ruby laser from the surface and the component scattered at an angle of 40 – 50°. Using the synchronisation of the Nd : YAG laser radiation, probing radiation, and the high-speed camera, we were able to obtain images of any stage of the melting process.

3. Experimental results and discussion

To reach the aim formulated above, first of all one should solve the problem of disturbing the melt stability at the radiation intensity exceeding the threshold value. This problem is of principal importance.

3.1. Buffer volume of the melt

The heating of metal by laser radiation is governed by heat conduction, heat transfer by convective Marangoni flows, and the deflection of the free-metal surface, which is accompanied by the formation of a vapour-gas channel and the displacement of an effective heat source deep into the melt bath. As the radiation intensity at the surface is increased, all other parameters being fixed, the first, second, and third of these mechanisms successively become of primary importance. A vapour-gas channel can arise only upon the formation of the so-called critical crater, when the deflection and the curvature of the melt surface reach the values providing multiple reflection of radiation from the crater walls, which is accompanied by a sharp increase in the portion of absorbed radiation energy.

As a result, the temperature and the pressure of a vapour-gas mixture are increased, which causes an ejection of droplets of the molten metal from the crater surface. The threshold radiation intensity is one of the main characteristics of metal melting by pulsed laser radiation. For chromium steel exposed to laser pulses of shape 1 (Fig. 2), the threshold intensity for metal injection was $q^* \simeq 8 \times 10^5$ W cm^{-2}.

Because a large depth of the melting zone in the case of a relatively small transverse size can be obtained only under the conditions when a vapour-gas channel is formed and grows, deep melting requires the fulfilment of two contradictory requirements. One should provide a sufficiently high pressure of a vapour-gas mixture in the growing channel and retain the melt stability, i. e., prevent the ejection of particles from a liquid metal under the action of vapour pressure. One of the possible ways of solving the deep-melting problem is to optimise the shape of laser pulses.

The study of irradiation of different steels and aluminium alloys in the above-threshold regime showed that the melting zone under these conditions was characterised by a considerably larger aspect ratio (~ 5) and a considerably larger depth than below the threshold. However, for almost all pulse shapes in the above-threshold regime, an intense melt ejection and the formation of a deep crater, which was elongated in the direction of the axis of the melting zone, were observed. The presence of an intense peak at the beginning or the end of a pulse results in the production of deepest craters in steel. The smoothing of pulse edges is accompanied by a decrease in the crater depth . However, a symmetric pulse is unable to suppress the ejection of liquid particles. A certain displacement of the peak to the trailing edge of a pulse (oscillograms 9 and 10, Fig. 2) enabled us to obtain a negligibly weak melt ejection. Using radiation pulses with a long leading edge, we obtained the melting zone 4.3 mm deep at an energy of 23.0 J. In this case, the threshold intensity was $q^* \simeq 2 \times 10^6$ W cm^{-2}. Thus, the optimisation of the shape of laser pulses should be considered as a possible way of increasing the depth to which the melting front penetrates due to an increase in the vapour-gas channel length. Note that such regimes favour the suppression of melt ejection from the heated region.

The high-speed photochronography showed that pulse of shape 9 (Fig. 2) with full duration of 12.0 ms and energy of 20 – 22 J formed on the surface of chromium steel a continuous film of the melt within 450 μs after the beginning of irradiation. During the first two milliseconds, the melting zone increased in diameter with a rate of 40 cm s^{-1}. Later on, this rate decreased down to 6.5 sm s^{-1}, and this value was retained till the end of the laser pulse. By the end of

the second millisecond of the melting process, a crater of critical depth was formed. The configuration of the inner region of the crater somewhat changed during the action of the radiation pulse, but its average transverse size remained approximately equal to 0.2 – 0.3 mm. The average diameter of the upper region of the vapour-gas channel did not exceed 0.10 – 0.12 mm.

The structure of convective flows in the melt bath, which are of substantial importance in heat and mass transfer, was studied in a separate series of experiments using transverse and longitudinal metallographic sections of a hardened melt in samples of commercially pure titanium irradiated in the nitrogen atmosphere. A thin titanium nitride layer, which is synthesised on the surface on the melt surface, was transferred by convective flows deep into the melting zone, so that we could obtain qualitative information on the flow structure from the position of regions enriched with TiN.

Fig. 3 shows the longitudinal sections of the melting zone for different radiation energies. One can see in Fig. 3a a residual deflection of the melt surface and two typical vortices, which represent the meridional section of closed Marangoni flows in a shallow bath. In Fig. 3b, these vortices are pronounced better. Moreover, one can clearly see a flow at the centre of the melting zone, which is directed downward along the z-axis and was formed under the action of the metal vapour recoil. It follows from Figs. 3c and 3d that the volume of the melt involved in the motion along the vertical axis rapidly increases with increasing radiation energy. The appearance of convective flows along the z-axis is caused by the formation and growth of the vapour-gas channel, which provides the displacement of the heat source from the irradiated surface deep into the melting zone.

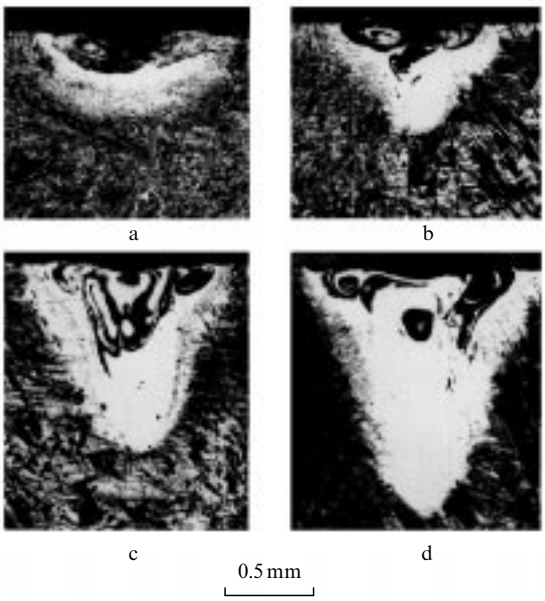

Figure 3. Convective flows in the melting zone (longitudinal section) at radiation energies of 1.3 (a), 5.6 (b), 8.4 (c), and 8.4 J (d).

Fig. 4 presents the transverse metallographic sections of a hardened melt at a depth of 0.2 mm. One can see that a large-scale vortex motion of a liquid metal is formed in the melting zone. A similar picture was observed for all the samples under study at the depth where the flows were preferentially oriented along the z-axis. In Ref. [14], the appearance of such vortex motion is related to the Rayleigh-Taylor instability of the melt motion along the z-axis in the field of surface tension forces, whose development time $t \approx 1/\gamma \approx 3 \times 10^{-3}$ s is determined by the increment $\gamma = \sqrt{g/d}$, where g is the acceleration caused by the surface tension forces and d is a typical size of the melt bath.

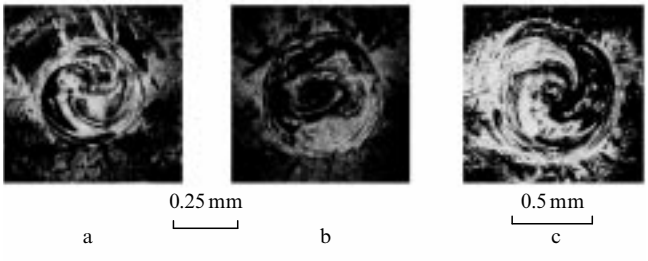

Figure 4. Convective flows in the melting zone (transverse region) at radiation energies of 3.4 (a), 4.3 (b), and 11.0 J (c).

Fig. 5 presents the dependences $t_m(z)$ and $V_f(z)$, which were experimentally observed by the technique described above for a series of 11 samples with the melting zone 3.2 ± 0.1 mm deep. One can see that the depth of the melting front during the most part of the irradiation time is not greater than 0.7 mm, whereas the melt bath deeper than 3 mm is formed in a time of about 2.5 ms. The velocity of motion of the melting front at the initial stage of growth of the vapour-gas channel length is about 1.0 m s^{-1}. One can also see from Fig. 5 that the rate of growth of the vapour-gas channel increases with increasing its length, and the strongest increase is observed at the final stage of the process at a depth greater than 2.5 mm.

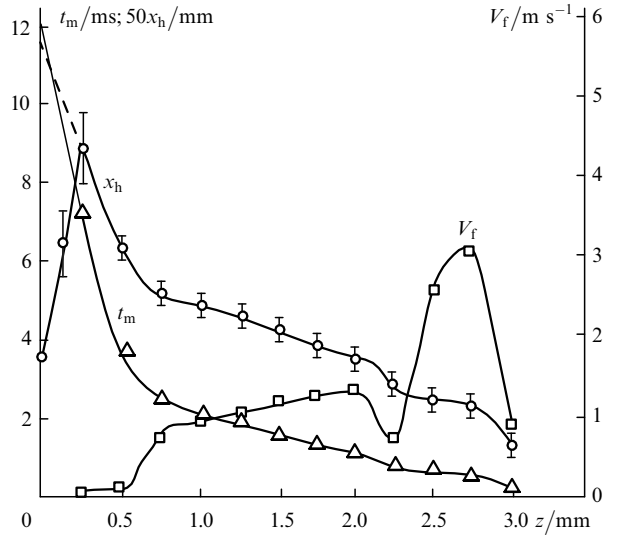

Figure 5. The hardening-layer thickness x_h, the melt lifetime t_m, and the melting-front velocity V_f as functions of the depth z.

Integrating the function $V_f(z)$, one can obtain the time dependence of the coordinate of the melting front $z_f(t)$ (Fig. 6). Here, we took into account the results of high-speed photochronography of melting, according to which a crater of critical depth ($z = 0.25$ mm) is formed by the end of the sec-

ond millisecond. One can see from Fig. 6 that a rapid growth in the length of the vapour-gas channels begins at a depth of 0.70 – 0.75 mm, 6.0 – 6.5 ms after the beginning of a laser pulse at the intensity $q \approx (0.9 - 1.0) \times 10^6$ W cm^{-2}. This process (the hatched region in Fig. 6) terminates at $q \approx 1.25 \times 10^6$ W cm^{-2}, and its duration is 2.5 ms. In view of the fact that the laser radiation intensity increases only slightly on this time interval, a considerable increase in the rate of growth of the vapour-gas channel during the increase in its length is of considerable interest. An increase in the laser radiation intensity at the bottom of the growing vapour-gas channel, which has been first experimentally realised in [13], was named the self-concentration of a heat source.

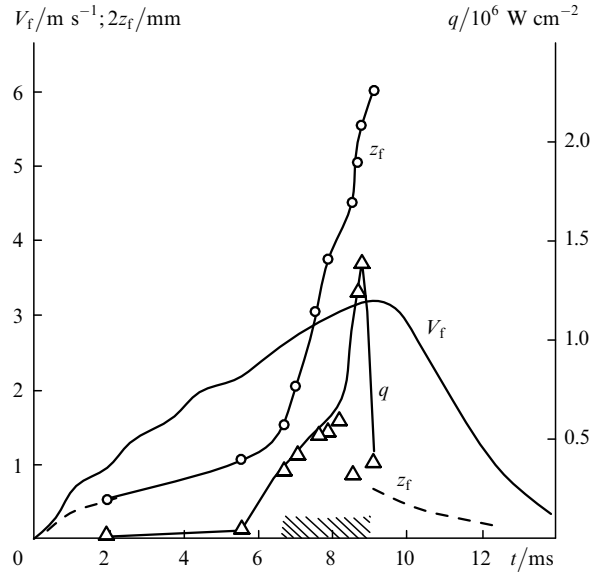

Figure 6. Coordinate z_f and the velocity V_f of the melting front as functions of time, and an oscillogram of a radiation pulse, q.

Fig. 7 illustrates the transformation of the shape of radiation pulses that corresponds to an increase in the energy from 23.0 to 34.0 J, with the focal region decreased in diameter from 0.32 to 0.29 mm. In the second case, the melting zone was 5.8 mm deep and the aspect ratio exceeded 5. The threshold intensity of the incident laser radiation was $q^* = 4 \times 10^6$ W cm^{-2}. In the experiments under consideration, it is appropriate to use the ratio of the melting-region depth to the radiation pulse energy $\eta = h/E$ as a characteristic of the energy deposition in a metal (the efficiency parameter). In the last of the aforementioned experiments, we had $\eta = 0.17$ mm J^{-1}.

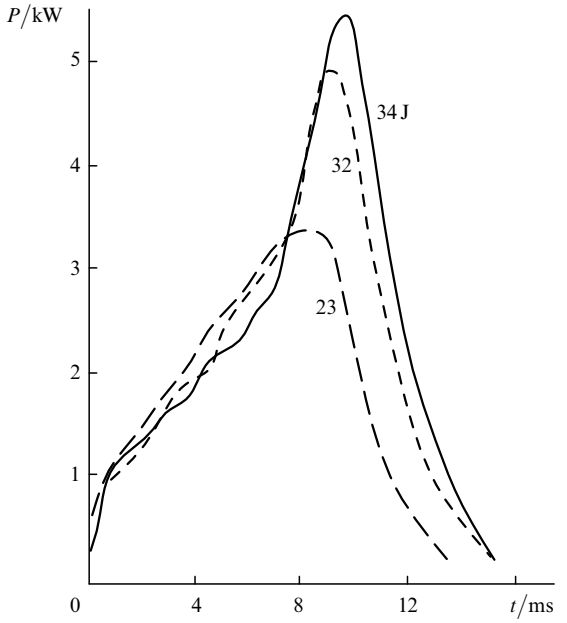

Figure 7. Shapes of the radiation pulse with the energy 23, 32, and 34 J.

Thus, it is reasonable to distinguish the following stages of steel melting by millisecond laser pulses:

(1) surface heating to the melting temperature and the formation of a visible film of a liquid metal (0.4 ms);

(2) a rapid growth of the melt volume and the formation of a crater of critical depth (2.0 ms);

(3) a slow increase in the melting zone in diameter, a non-monotone increase of the crater depth, which is accompanied by the development of the Rayleigh-Taylor instability, and the formation of a primary capillary (5.5 – 6.0 ms);

(4) an increase in the vapour-gas channel in length with an increasing rate because of the self-concentration of a heat source, and the formation of the melting zone of maximum depth (9.0 – 9.2 ms);

(5) the disappearance of the vapour-gas channel and the heating of the upper part of the melt bath by the trailing edge of a radiation pulse (12.0 ms).

The analysis of many experiments performed at near-threshold radiation intensities showed that one can retain the melt stability during the crater formation and the growth of the vapour-gas channel in length if an initial melt bath with a sufficiently large volume, which was named in Ref. [14] the buffer volume, was formed before the deflection of the melt surface. The buffer volume is formed under the action of laser radiation of relatively low intensity, which corresponds to the extended leading edge of a radiation pulse.

3.2. The effect of spatial radiation parameters on characteristics of the melting process

The analysis of laser radiation distributions in a hollow vapour-gas channel shows that the radiation loss depends on the solid angle enclosing the region of radiation propagation behind the focusing objective (the aperture angle β_0). Its decrease corresponds to a decrease in loss [13]. The aperture angle and the laser radiation intensity on the irradiated surface are determined by the direct-beam aperture A_0, the objective focal distance F, the laser radiation divergence θ_0, and the telescope magnification K, in accordance with (2). Table 1 presents the depth of the melting zone h as a function of β_0 and d in two experiments with $2\theta_0 = 8.0$ mrad, $2A_0 = 6.0$ mm ($F = 100$ mm) and $2\theta_0 = 4$ mrad, $2A_0 = 3.0$ mm ($F = 150$ mm). In both cases, we used the same radiation energy of 12 – 13 J. Regimes 1 – 3 differ from the rest regimes by the fact that in the latter cases we decreased both the divergence and the aperture of a laser beam. As a result, the melting depth in regimes 4 – 7 is noticeably larger than in regimes 1 – 3, the energy deposition being fixed.

Worthy of notice is regime 5 with $d = 0.18$ mm and $2\beta_0 = 0.07$ in which we obtained the melting depth as large as 5.5 mm at a relatively low radiation energy (12.5 J). As the energy is increased, the requirement of retaining the melt stability leads, as noted above, to the necessity of lengthening

Table 1. Dependence of the melting depth h on the irradiation region diameter p and the aperture angle β_0.

Regime number	d/mm	$2\beta_0$/rad	h/mm
1	0.20	0.24	2.0
2	0.40	0.12	2.4
3	0.80	0.06	0.9
4	0.14	0.09	1.5
5	0.18	0.07	5.5
6	0.24	0.05	3.5
7	0.32	0.04	2.9

the leading edge of a radiation pulse (curve of 34 J in Fig. 7). As a result, we obtained a melting depth of 6.5 mm at an energy of 17.5 J. In this case, the aspect ratio of the melting zone is about 15, which is more typical for the electron-ray welding. The threshold intensity in regime 5 was 6×10^6 W cm^{-2}, which exceeds the corresponding value for unoptimised radiation parameters by a factor of about ten. In this regime, the efficiency factor is about 0.4 mm J^{-1}.

A change in the aperture angle and the focal-region diameter has a substantial effect on the dynamic parameters of the growth of the vapour-gas channel. Fig. 8a presents the dependences of the growth rate of the vapour-gas channel length on the melting depth for $K = 7.2$ and 10.8. One can see that in both cases the rate considerably increases during the growth of the vapour-gas channel. In Fig. 8b, the same dependences are plotted in the rate-time coordinates. One can see that the curve for the regime with $K = 10.8$ is almost coincident with the final segment of the curve for $K = 7.2$. The lifetime of the vapour-gas channel in the regime with $K = 10.8$ was 0.9 ms. In this case, the laser radiation intensity at the surface was too low for obtaining a large melting depth. However, owing to the fact that the aperture angle was sufficiently small, the self-concentration of a heat source leads to the formation of a vapour-gas channel at a later stage and its increase in length.

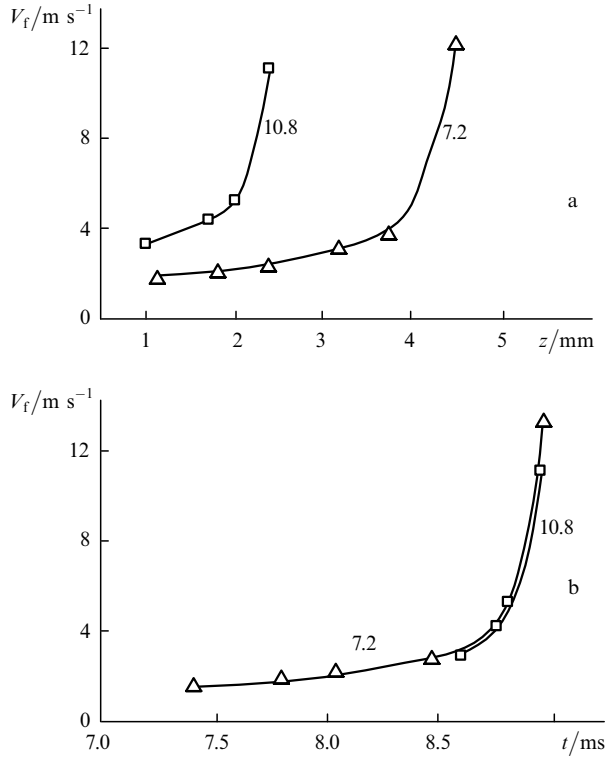

Figure 8. The rate of growth of the vapour-gas channel length as a function of melting depth (a) and time (b) for $K = 7.2$ and 10.8.

Our experiments showed that the self-concentration of a heat source during its development leads at a certain stage of the melting process to pure evaporation and the formation of narrow cavities that are not filled with a melt. A jump in the rate of channel growth above 10 m s^{-1} corresponds to the presence of such cavities. Here, the channel lifetime for the regime with $K = 10.8$ is 5×10^{-5} s. In our experiments, the lower part of a cavity was 10 – 20μm in diameter. In this case, a channel should be treated as a hollow metal waveguide.

3.3. Waveguide propagation of radiation in a vapour-gas channel

The authors of Ref. [17] studied experimentally the effect of spatial parameters of a laser beam with the wavelength λ_0 on the efficiency and the dynamic parameters of steel melting under conditions where the diameter d of a vapour-gas channel was sufficiently small and its length L was sufficiently large, so that $d^2/\lambda_0 \ll L$ and the waveguide propagation of radiation in a channel was realised. The dependences of the melting-region depth h on the energy E for θ and β that were varied by changing the telescope magnification, were found to be well approximated by linear functions.

As the divergence is decreased from 2.20 to 0.50 mrad, the coefficient η increases. However, η begins to decrease with a further decrease in the divergence from 0.30 to 0.17 mrad; the corresponding decrease is observed for the melting depth. The analysis of the dependence of the coefficient η on the beam divergence, with aperture angles being fixed, showed that the maximum efficiency $\eta \sim 0.5$ mm J^{-1} was reached in the interval 0.05 rad $< \beta <$ 0.1 rad; the average aperture angle corresponding to the maximum efficiency was 0.075 – 0.080 rad.

The presence of an extremum in the dependence of the melting efficiency on the aperture angle is not obvious because it follows from the geometric analysis [15, 16] that the efficiency of radiation transfer to the bottom of a vapour-gas channel should monotonically increase with decreasing aperture angle β. The coefficient of reflection from a smooth metal surface has the form [4]

$$R = -\left(\frac{2\omega}{\pi\sigma}\right)^{1/2} \cos\left(\frac{\pi}{2} - \beta\right),$$

where σ is the conductivity and ω is the plasma frequency. As β is decreased, the coefficient of laser radiation reflection from the walls of a vapour-gas channel monotonically increases, and the effective number of reflections required to reach the bottom of a channel decreases.

The propagation of an electromagnetic wave in a metal capillary was studied in detail in [18, 19]. Substituting the average aperture angle $\beta \approx 0.08$ rad corresponding to the maximum of the efficiency parameter in the expression for the minimum of the damping coefficient of the H mode ($\beta \approx 1/\sqrt{kr_0}$), we obtain the following estimate for the vapour-gas channel radius:

$$r_0 \approx 1/k\beta^2 \approx 25\ \mu\text{m}, \quad (6)$$

where k is the wave number. This estimate agrees well with a value of 10 – 30 μm that was presented above for the diameter of the channel in its narrowest region.

Thus, the waveguide approximation adequately describes the propagation of radiation in a vapour-gas channel in our experiments. It describes the experimental dependence of the efficiency parameter of melting on the aperture angle. The aperture angle found in the experiments and corresponding to the maximum of the parameter η ($\beta \approx 0.075 - 0.08$ rad) should be considered as an optimum angle in the determination of conditions of pulsed laser welding and the designing of technological laser systems.

It follows from the experimental results presented above that the beam quality parameter $\theta_0 A_0$, which is often used as a characteristic of laser radiation, is insufficient for the analysis of radiation transport in a vapour-gas channel. As follows from the aforesaid, the aperture and the divergence of a laser beam should be independently optimised in this case. Nevertheless, it is of interest for practice to determine, starting from the parameters of series-produced technological systems, the limiting values of the parameter $\theta_0 A_0$ required for obtaining deep melting. One can easily find from relation (4) the expression determining the beam quality parameter:

$$\theta_0 A_0 = \frac{1}{2}\beta d. \quad (7)$$

Taking into account that the focal region should be not larger than 0.3 mm in diameter, one can easily find from (7) that the beam quality parameter should not exceed 12 mm×mrad, provided the aperture angle is close to the optimum value. For a standard active element 6.3 mm in diameter, this corresponds to the incident-beam divergence of about 2 mrad. Note that industrial pulsed Nd:YAG lasers typically have $\theta_0 A_0 \approx 40 - 60$ mm mrad.

4. Requirements to a pulsed laser for deep welding of metals

(1) The design of a pump source should provide the feasibility of smooth tailoring of the radiation pulse shape. The optimisation of the pulse shape predominantly consists in the choice of duration of the leading edge of a pulse, radiation intensity on this interval, duration of the main peak of the pulse, and its intensity. The leading edge of the pulse and its main peak should produce the radiation intensities on the surface being processed equal to $\sim 10^5$ and $10^6 - 10^7$ W cm^{-2}, respectively.

(2) The control of the full duration of radiation pulses from 2 to 20 ms should be provided.

(3) The aperture of a laser beam incident on an objective and its focal distance should be chosen in a way providing an optimum aperture angle of 0.075 – 0.080 rad.

(4) A laser beam should have a sufficiently low divergence, so that the diameter of the irradiation region for an optimum aperture angle be not greater than 0.3 mm. For an active element 6.3 mm in diameter, the divergence should not exceed 2 mrad.

(5) The maximum radiation intensity in a pulse should be not lower than h/η, where h is the desired melting depth and η is the efficiency parameter corresponding to the prescribed radiation parameters and the material of details being welded.

5. Conclusions

Thus, we have experimentally substantiated the role of the buffer melt volume in the suppression of ejection of a liquid metal from the laser-heated region with a deflected melt surface and in the growth of a vapour-gas channel. For pulsed lasers operating in the near IR region, the self-concentration of a heat source at the bottom of a vapour-gas channel during its growth was realised. For millisecond laser pulses with energy below 20 J, the melting zone as deep as 6 mm was obtained, which exceeds the value that was previously thought to be the maximum possible depth by a factor of about three.

The dependences of the efficiency parameter, the melting depth, and the rate of growth of the vapour-gas channel in length on the aperture angle β under the experimental conditions providing a rapid growth of the vapour-gas channel length and, therefore, a large melting depth were found to have an extremum. The maximum values of these parameters were achieved at $\beta = 0.080 - 0.075$ rad. The efficiency parameter as large as $\eta \approx 0.5$ mm J^{-1} has been first obtained for millisecond laser pulses. The requirements to pulsed laser technological systems providing high-quality deep welding of metals were formulated.

References

1. Anisimov S I, Imas Ya A, Romanov G S, Khodyko Yu V *Deistvie Izlucheniya Bol'shoi Moshchnosti na Metally* (The Action of High-Power Radiation on Metals) (Moscow: Nauka, 1970)
2. Rykalin N N, Uglov A A, Zuev I V, Kokora A N *Lazernaya i Elektronno-Luchevaya Obrabotka Materialov* (Laser and Electron-Beam Metal Processing) (Moscow: Mashinostroenie, 1985)
3. Grigor'yants A G *Osnovy Lazernoi Obrabotki Materialov* (Foundations of Laser Material Processing) (Moscow: Mashinostroenie, 1989)
4. Vedenov A A, Gladush G G *Fizicheskie Protsessy pri Lazernoi Obrabotke Materialov* (Physical Processes in Laser Material Processing) (Moscow: Energoatomizdat, 1985)
5. Locke E V, Hoag E D, Hella R A *IEEE J. Quantum Electron.* **8** 601 (1972)
6. Basov N G, Bashenko V V, Glotov E N, Gornyi S G, Danilychev V A, Karpov E N, Lopota V A, Malysh M M, Rudoi N G, Saburov V A *Izv. Akad Nauk SSSR Ser. Fiz.* **48** 2310 (1984)
7. Gornyi S G, Lopota V A, Soroka A M *Materialy Mezhdunarodnoi Konferentsii 'Lazery v Narodnom Khozyaistve'* (Technical Digest of the International Conference 'Lasers in Industry') (Moscow, 1986) p. 7
8. Carslaw H S, Jaeger J C *Conduction of Heat in Solids* (Clarendon Press: Oxford, 1959)
9. Kayukov S V, Gusev A A, Nesterov I G, Zaichikov E G, Petrov A L *Proceedings of the International Conference on New Advances in Welding and Allied Processes* (Beijing, 1991) Vol. 1, p. 183
10. Bransch H N, Wang Z Y, Liu L T, Weckman D C, Kerr H W J. *Laser Appl.* **3** (3) 25 (1991)
11. Kayukov S V, Gusev A A *Kvantovaya Elektron.* **22** 811 (1995) [*Quantum Electron.* **25** 780 (1995)]
12. Kayukov S V, Gusev A A, Nesterov I G, Zaichikov E G, Petrov A L *Fiz. Khim. Obrab. Mater.* **4** 36 (1996)
13. Kayukov S V, Gusev A A *Kvantovaya Elektron.* **23** 711 (1996) [*Quantum Electron.* **26** 692 (1996)]
14. Kayukov S V, Gusev A A *Kvantovaya Elektron.* **23** 1025 (1996) [*Quantum Electron.* **26** 999 (1996)]
15. Kayukov S V, Gusev A A, Zaichicov E G, Petrov A L *Laser Phys.* **8** 527 (1998)
16. Solana P, Negro G *J. Phys. D* **30** 3216 (1997)

17. Kayukov S V, Gusev A A *Kvantovaya Elektron.* **30** 337 (2000) [*Quantum Electron.* **30** 337 (2000)]
18. Bol'shov L A, Krivoruchko K A, Reshetin V P *Preprint No. 6/1985* (Minsk: ITMO, 1985)
19. Arutyunyan R V, Baranov V Yu, Bol'shov L A, Malyuta D D, *Sebrant A Yu Vozdeistvie Lazernogo Izlucheniya na Materialy* (The Action of Laser Radiation on Materials) (Moscow: Nauka, 1989)